Steel and Composite Structures, *Vol. 35, No. 5 (2020) 635-640*
DOI: https://doi.org/10.12989/scs.2020.35.5.635

Buckling analysis of smart beams based on higher order shear deformation theory and numerical method

Pouyan Talebizadehsardari[1,2a], Arameh Eyvazian[3], Mojtaba Gorji Azandariani[4], Trong Nhan Tran[5], Dipen Kumar Rajak[6] and Roohollah Babaei Mahani[*7,8]

[1]*Metamaterials for Mechanical, Biomechanical and Multiphysical Applications Research Group, Ton Duc Thang University, Ho Chi Minh City, Vietnam*
[2]*Faculty of Applied Sciences, Ton Duc Thang University, Ho Chi Minh City, Vietnam*
[3]*Mechanical and Industrial Engineering Department, College of Engineering, Qatar University, P.O. Box 2713, Doha, Qatar*
[4]*Structural Engineering Division, Faculty of Civil Engineering, Semnan University, Semnan, Iran*
[5]*Faculty of Automobile Technology, Van Lang University, Ho Chi Minh City, Vietnam*
[6]*Department of Mechanical Engineering, Sandip Institute of Technology and Research Centre, Nashik 422213, MH-India*
[7]*Institute of Research and Development, Duy Tan University, Da Nang 550000, Vietnam.*
[8]*Faculty of Civil Engineering, Duy Tan University, Da Nang 550000, Vietnam*

(*Received April 1, 2020, Revised May 17, 2020, Accepted May 26, 2020*)

Abstract. The buckling analysis of the embedded sinusoidal piezoelectric beam is evaluated using numerical method. The smart beam is subjected to external voltage in the thickness direction. Elastic medium is simulated with two parameters of spring and shear. The structure is modelled by sinusoidal shear deformation theory (SSDT) and utilizing energy method, the final governing equations are derived on the basis of piezo-elasticity theory. In order to obtaining the buckling load, the differential quadrature method (DQM) is used. The obtained results are validated with other published works. The effects of beam length and thickness, elastic medium, boundary condition and external voltage are shown on the buckling load of the structure. Numerical results show that with enhancing the beam length, the buckling load is decreased. In addition, applying negative voltage, improves the buckling load of the smart beam.

Keywords: smart beam; buckling; SSDT; numerical method; elastic medium

1. Introduction

Nanocomposite structures are made from a matrix reinforced with nanoparticles for improving the property of the material. Recently, the properties of nanocomposite structures have encouraged researchers to investigate about these materials. These structures have many applications such as producing batteries with greater power output, speeding up the healing process for broken bones, producing structural components with a high strength-to-weight ratio, structures and so on.

Buckling analysis of composite structures has been presented by many researchers. Bending and local buckling of a nanocomposite beam reinforced by a single-walled carbon nanotube (SWCNT) were studied by Vodenitcharova and Zhang (2006) based on the Airy stress-function method. Buckling analysis of nanocomposite Timoshenko beams reinforced by SWCNTs resting on an elastic foundation was investigated by Yas and Samadi (2012) using the generalized differential quadrature method (GDQM). Kolahchi *et al.* (2015) investigated nonlocal nonlinear buckling analysis of temperature-dependent microplates reinforced with FG-SWCNT resting on an elastic matrix as orthotropic temperature-dependent elastomeric medium. Based on harmonic differential quadrature (HDQ), Mehri *et al.* (2016) analyzed buckling and vibration responses of a composite truncated conical shell with embedded SWCNTs subjected to an external pressure and axial compression simultaneously. Buckling and vibration analysis of cantilever functionally graded (FG) beam that reinforced with carbon nanotube (CNT) were presented by Nejati *et al.* (2016). In this paper, an equivalent continuum model based on the Eshelby–Mori–Tanaka approach was obtained. Based on DQM and Bolotin's method, Kolahchi *et al.* (2016a,b) investigated nonlinear dynamic buckling analysis of embedded temperature-dependent viscoelastic plates reinforced by SWCNTs. Mosharrafian and Kolahchi (2016) presented buckling analysis of classical piezoelectric polymeric cylindrical shell reinforced by armchair double walled boron nitride nanotubes (DWBNNTs). The free vibration and linearized buckling analysis of laminated composite plates were studied using the Isogeometric approach (IGA) and Carrera's Unified Formulation (CUF) (Alesadi *et al.* 2017). Yang *et al.* (2017) studied buckling and postbuckling behaviours of functionally graded multilayer nanocomposite beams reinforced with a low content of graphene platelets (GPLs) resting on an elastic foundation. It was assumed that GPLs are randomly oriented and uniformly dispersed in each individual GPL-

∗Corresponding author, Ph.D.
E-mail: roohollahbabaeimahani@duytan.edu.vn
[a] E-mail: ptsardari@tdtu.edu.vn".

Copyright © 2020 Techno-Press, Ltd.

ISSN: 1229-9367 (Print), 1598-6233 (Online)

reinforced composite (GPLRC) layer with its weight fraction varying layerwise along the thickness direction. Zamanian *et al.* (2017) investigated buckling of an embedded straight beams reinforced with silicon dioxide (SiO2) nanoparticles based on Euler- Bernoulli and Timoshenko beam models. The nonlinear buckling of straight beams armed with SWCNTs resting on foundation was investigated by Bilouei *et al.* (2016) using DQM. Khelifa *et al.* (2018) presented a multi-layer finite element for buckling and free vibration analyses of laminated beams based on a higher-order layer-wise theory. The influence of the initial lateral (sweep) shape and the cross-sectional twist imperfection on the lateral torsional buckling (LTB) response of doubly-symmetric steel I-beams was investigated by Benahmed *et al.* (2019). Post-buckling of a cut out plate reinforced through carbon nanotubes (CNTs) resting on an elastic foundation was studied by Motezaker and Eyvazian (2020a). In another work by the same authors, buckling and optimization of a nanocomposite beam was studied by Motezaker and Eyvazian (2020b). Eltaher and Mohamed (2020) presented a comprehensive model to study static buckling stability and associated mode-shapes of higher shear deformation theories of sandwich laminated composite beam under the compression of varying axial load function.

However, to date, no research about the buckling of smart beam with mathematical models has been found in the literature. For the first time, buckling analysis of embedded smart beams under the buckling constraint is presented in this present work. The SSDT is used for modeling of structure and the corresponded governing equations are derived by energy method and Hamilton's principal. Using DQM, the buckling load of structure is calculated. The effects of the axial forces, applied voltage, beam length and thickness, spring constant and shear constant of foundation on the buckling load are studied.

2. Formulation

A smart beam with the length of *L* and cross section of $b \times h$ is shown in Fig. 1, where the structure is subjected to external applied voltage in thickness direction and surrounded by elastic foundation.

Using SSDT, the displacement field can be written as (Thai and Vo 2012)

$$u_1(x,z,t) = u(x,t) - z\frac{\partial w(x,t)}{\partial x} + f\psi(x,t), \quad (1)$$

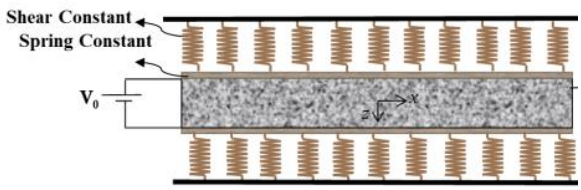

Fig. 1 The schematic view of the nanocomposite beam

$$u_2(x,z,t) = 0, \quad (2)$$

$$u_3(x,z,t) = w(x,t), \quad (3)$$

where, u_1 u_2 and are the displacement of the u_3 mid plane in the axial, transverse and thickness directions; ψ represents the rotation of cross section about *y* axis; $f = \frac{h}{\pi}\sin\left(\frac{\pi z}{h}\right)$. Using Eqs. (1) to (3), the nonlinear strain-displacement relations based on Von -Karman theory are as follows

$$\varepsilon_{xx} = \frac{\partial u}{\partial x} - z\frac{\partial^2 w}{\partial x^2} + \frac{1}{2}\left(\frac{\partial w}{\partial x}\right)^2 + f\frac{\partial \psi}{\partial x}, \quad (4)$$

$$\varepsilon_{xz} = \cos\left(\frac{\pi z}{h}\right)\psi. \quad (5)$$

In piezoelectric material, stress (σ) and the strain (ε) from the side with an electrical displacement (D) and electric field (E) from the electrostatic side can be coupled as follows (Kolahchi *et al.* 2016a)

$$\begin{bmatrix}\sigma_{xx}\\ \sigma_{yy}\\ \sigma_{zz}\\ \tau_{yz}\\ \tau_{xz}\\ \tau_{xy}\end{bmatrix} = \begin{bmatrix}Q_{11} & Q_{12} & Q_{13} & 0 & 0 & 0\\ Q_{12} & Q_{22} & Q_{23} & 0 & 0 & 0\\ Q_{13} & Q_{23} & Q_{33} & 0 & 0 & 0\\ 0 & 0 & 0 & Q_{44} & 0 & 0\\ 0 & 0 & 0 & 0 & Q_{55} & 0\\ 0 & 0 & 0 & 0 & 0 & Q_{66}\end{bmatrix}\begin{Bmatrix}\varepsilon_{xx}\\ \varepsilon_{yy}\\ \varepsilon_{zz}\\ \gamma_{yz}\\ \gamma_{xz}\\ \gamma_{xy}\end{Bmatrix} - \begin{bmatrix}0 & 0 & e_{31}\\ 0 & 0 & e_{32}\\ 0 & 0 & e_{33}\\ 0 & e_{24} & 0\\ e_{15} & 0 & 0\\ 0 & 0 & 0\end{bmatrix}\begin{Bmatrix}E_x\\ E_y\\ E_z\end{Bmatrix}, \quad (6)$$

$$\begin{bmatrix}D_x\\ D_y\\ D_z\end{bmatrix} = \begin{bmatrix}0 & 0 & 0 & 0 & e_{15} & 0\\ 0 & 0 & 0 & e_{24} & 0 & 0\\ e_{31} & e_{32} & e_{33} & 0 & 0 & 0\end{bmatrix}\begin{Bmatrix}\varepsilon_{xx}\\ \varepsilon_{yy}\\ \varepsilon_{zz}\\ \gamma_{yz}\\ \gamma_{xz}\\ \gamma_{xy}\end{Bmatrix} + \begin{bmatrix}\in_{11} & 0 & 0\\ 0 & \in_{22} & 0\\ 0 & 0 & \in_{33}\end{bmatrix}\begin{Bmatrix}E_x\\ E_y\\ E_z\end{Bmatrix}, \quad (7)$$

where Q_{ij}, e_{ij} and $\in_{ij}$ are elastic, piezoelectric and dielectric constants, respectively. The electric field (E_k) in terms of electric potential is defined as follows

$$E_k = -\nabla\Phi,$$

where the electric potential distribution is assumed as follows (Kolahchi *et al.* 2016a)

$$\Phi(x,z,t) = -\cos\left(\frac{\pi z}{h}\right)\varphi(x,t) + \frac{2V_0 z}{h}. \quad (8)$$

where V_0 is the external voltage. However, based on SSDT (Thai and Vo 2012), Eqs. (13) and (14) can be simplified as

$$\sigma_{xx} = Q_{11}\left(\frac{\partial u}{\partial x} - z\frac{\partial^2 w}{\partial x^2} + f\frac{\partial \psi}{\partial x}\right) + e_{31}\left(\frac{\pi}{h}\sin\left(\frac{\pi z}{h}\right)\phi + \frac{2V_0}{h}\right). \quad (9)$$

$$\sigma_{xz} = Q_{55}\left(\cos\left(\frac{\pi z}{h}\right)\psi\right) - e_{15}\left(\cos\left(\frac{\pi z}{h}\right)\frac{\partial\phi}{\partial x}\right), \quad (10)$$

$$D_x = e_{15}\left(\cos\left(\frac{\pi z}{h}\right)\psi\right) + \in_{11}\left(\cos\left(\frac{\pi z}{h}\right)\frac{\partial\phi}{\partial x}\right), \quad (11)$$

$$D_z = e_{31}\left(\frac{\partial u}{\partial x} - z\frac{\partial^2 w}{\partial x^2} + f\frac{\partial\psi}{\partial x}\right) - \in_{33}\left(\frac{\pi}{h}\sin\left(\frac{\pi z}{h}\right)\phi + \frac{2V_0}{h}\right), \quad (12)$$

where u and w are the displacement of the mid plane in the axial and thickness directions; ψ represents the rotation of cross section about *y* axis; $f = \frac{h}{\pi}\sin\left(\frac{\pi z}{h}\right)$.

The potential energy of structure can be written as follows

$$U = \frac{1}{2}\int_V \begin{pmatrix} \sigma_{xx}\left(\frac{\partial u}{\partial x} - z\frac{\partial^2 w}{\partial x^2} + \frac{1}{2}\left(\frac{\partial w}{\partial x}\right)^2 + f\frac{\partial\psi}{\partial x}\right) \\ +\sigma_{xz}\left(\cos\left(\frac{\pi z}{h}\right)\psi\right) - D_x\left(\cos\left(\frac{\pi z}{h}\right)\frac{\partial\phi}{\partial x}\right) \\ -D_z\left(-\frac{\pi}{h}\sin\left(\frac{\pi z}{h}\right)\phi - \frac{2V_0}{h}\right) \end{pmatrix} dV. \quad (13)$$

The external work due to the foundation around the beams can be expressed as (Kolahchi *et al.* 2015):

$$W = \int_x \left(-k_w w + k_g \nabla^2 w\right) w dx. \quad (14)$$

where k_w and k_g respectively are spring and shear constants. However, using Hamilton's principle, the governing equations can be expressed as

$$\delta u : \frac{\partial^2 u}{\partial x^2} + \frac{\partial w}{\partial x}\frac{\partial^2 w}{\partial x^2} = 0, \quad (15)$$

$$\begin{aligned} \delta w : & -Q_{11} I \frac{\partial^4 w}{\partial x^4} + \frac{24 Q_{11} I}{\pi^3}\frac{\partial^3 \psi}{\partial x^3} \\ & -\left(2e_{31}V_0 + N_x^M\right)\frac{\partial^2 w}{\partial x^2} - k_w w + k_g \nabla^2 w = 0, \end{aligned} \quad (16)$$

$$\begin{aligned} \delta\psi : & -\frac{24 Q_{11} I}{\pi^3}\frac{\partial^3 w}{\partial x^3} + \frac{6 Q_{11} I}{\pi^2}\frac{\partial^2 \psi}{\partial x^2} \\ & + \frac{e_{31} h}{2}\frac{\partial\phi}{\partial x} - \frac{Q_{55} A}{2}\psi + \frac{e_{15} h}{2}\frac{\partial\phi}{\partial x} = 0, \end{aligned} \quad (17)$$

$$\begin{aligned} \delta\phi : & -\frac{2h}{\pi}\frac{\partial^2 w}{\partial x^2} + \frac{h}{2}\frac{\partial\psi}{\partial x} - \frac{\pi^2 \in_{33}}{2h}\phi \\ & + \frac{h}{2}\frac{\partial\psi}{\partial x} + \frac{h \in_{11}}{2}\frac{\partial^2\phi}{\partial x^2} = 0. \end{aligned} \quad (18)$$

In the above equations, N_x^M is the internal applied force to the beam.

3. DQM

DQM is a numerical method which changes the differential equations to algebraic equations using weighting coefficients. Thus, at any point, derived as a linear sum of the weighted coefficients and values of the function at that point and other points in the direction of the axis will be expressed. The main relationship of DQM, can be expressed as follows (Kolahchi *et al.* 2016a, b):

$$\frac{df}{dx}\overset{x=x_i}{\rightarrow} = \sum_{j=1}^{N} C_{ij} f_j, \quad (19)$$

So that $f(x)$ is a function, N is the number of grid points and C_{ij} presents weighting coefficients. The roots of the polynomial Chebyshev heavily used in solving engineering problems and bring good results. Of separation is expressed as follows

$$X_i = \frac{L}{2}\left[1 - \cos\left(\frac{i-1}{N-1}\right)\pi\right] \quad i = 1,...,N. \quad (20)$$

With the roots of polynomial Lagrange transferred as the algebraic relations for calculating the weighting coefficients obtained

$$C_{ij}^{(1)} = \frac{L_1(x_i)}{(x_i - x_j)L_1(x_j)} \qquad for \quad i \neq j, \quad i, j = 1,2,...,N, \quad (21)$$

$$C_{ii}^{(1)} = -\sum_{j=1, j\neq i} C_{ij}^1 \qquad for \quad i = j, \ i = 1,2,...,N, \quad (22)$$

In these two equations

$$L(x_i) = \prod_{\substack{j=1 \\ j\neq i}}^{N_x} (x_i - x_j). \quad (23)$$

And for higher derivative, we have

$$C_{ij}^{(n)} = n\left(C_{ii}^{(n-1)} C_{ij}^{(1)} - \frac{C_{ij}^{(n-1)}}{(x_i - x_j)}\right) \qquad i \neq j. \quad (24)$$

Boundary condition equations are

- **Clamped- Clamped (CC)**

$$\begin{aligned} & w = u = \phi = \psi = \frac{\partial w}{\partial x} = 0, && @ \quad x = 0 \\ & w = u = \phi = \psi = \frac{\partial w}{\partial x} = 0. && @ \quad x = L \end{aligned} \quad (25)$$

- **Clamped- Simple (CS)**

$$\begin{aligned} & w = u = \phi = \psi = \frac{\partial w}{\partial x} = 0, && @ \quad x = 0 \\ & w = u = \phi = \frac{\partial \psi}{\partial x} = \frac{\partial^2 w}{\partial x^2} = 0. && @ \quad x = L \end{aligned} \quad (26)$$

- **Simple- Simple (SS)**

$$w = u = \phi = \frac{\partial \psi}{\partial x} = \frac{\partial^2 w}{\partial x^2} = 0, \quad @ \quad x = 0$$
$$w = u = \phi = \frac{\partial \psi}{\partial x} = \frac{\partial^2 w}{\partial x^2} = 0. \quad @ \quad x = L \tag{27}$$

Boundary condition equations due to having weight coefficients, equations are coupled ruling. As a result of the boundary condition and the field should be separated from each other. The governing equations and boundary conditions can be written in matrix form as follows

$$\left(\left[\underbrace{K_L + K_{NL}}_{K} \right] + P\left[K_g\right] \right) \begin{Bmatrix} \{d_b\} \\ \{d_d\} \end{Bmatrix} = 0, \tag{28}$$

In these relationships, P is the buckling load. Also, $[K_L]$, $[K_{NL}]$ and $[K_g]$ respectively, represents the stiffness matrix linear, nonlinear part of stiffness matrix and geometric matrix . However, using eigenvalue problem, the buckling load of structure can be obtained.

4. Numerical results

In this chapter, using the DQM, buckling load of the structure is calculated and the effect of various parameters are examined. For this purpose, a bam made from ZnO is selected with elastic constants of $Q_{11} = 207\ GPa$ and $Q_{55} = 44.6\ GPa$, piezoelectric constants of $e_{31} = -0.51\ C/m^2$ and $e_{15} = -0.45\ C/m^2$ and dielectric constants of $\in_{11} = 7.77 \times 10^{-8}\ F/m$ and $\in_{33} = 8.91 \times 10^{-8}\ F/m$. It should be noted that buckling load provided in this section, is dimensionless ($P = N_x^M/(C_{11}h)$).

Fig. 2 represents the structural buckling load of beam versus the mode number for different DQ grid points. As can be seen, with increasing the number of grid points, the buckling load decreases as far as in $N = 15$, it is converged. So the calculations in the project are done with 15 grid points.

Buckling of smart beams has not been studied by any researcher. So to verify our results, eliminating the effects foundations ($k_w = k_g = 0$) and piezoelectric properties, buckling analysis of a beam with SSDT is discussed. Considering the material and the geometric parameters similar to Thai and Vo (2012), buckling load was shown for different aspect ratios of structure in Table 1. As can be observed, the results of the present work in accordance with reference Thai and Vo (2012) show that the results are accurate. It should be noted that the small difference between current results and reference Thai (2012) is due to the difference in type theory. In this project, SSDT is used while in Thai (2012), Timoshenko beam theory is applied.

The effect of beam thickness on the dimensionless buckling load of the structure versus the number of longitudinal mode is shown in Fig. 3.

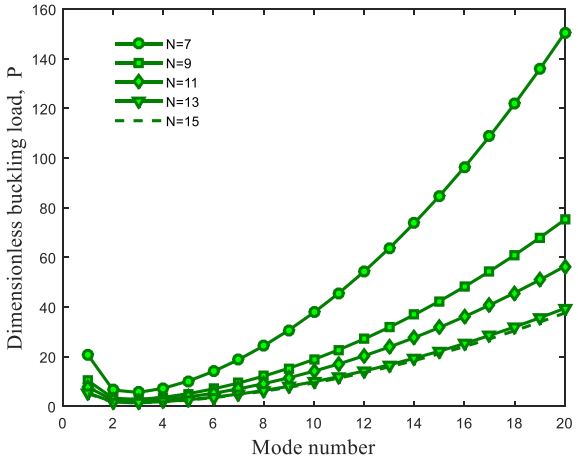

Fig. 2 Convergence and accuracy of DQM

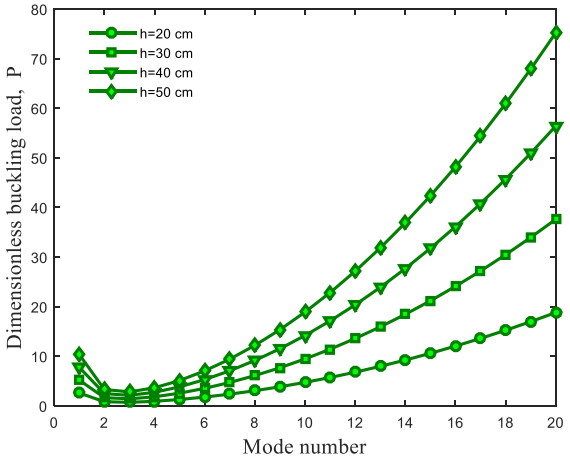

Fig. 3 Beam thickness effect on the dimensionless buckling load versus mode number

Table 1 Validation of present work with other published works

L/h	TBT, Thai (2012)	SSDT, Thai and Vo (2012)	SSDT, present
5	8.9509	8.9533	8.9532
10	9.6227	9.6232	9.6231
20	9.8067	9.8068	9.8068
10	9.8671	9.8671	9.8671
0			

To the point where it is minimal buckling load, is said to be critical buckling load. The critical buckling is reached in third longitudinal mode. Moreover, increasing the beam thickness increases the buckling load of beam. The reason for this is that by increasing the beam thickness, the stiffness is enhanced.

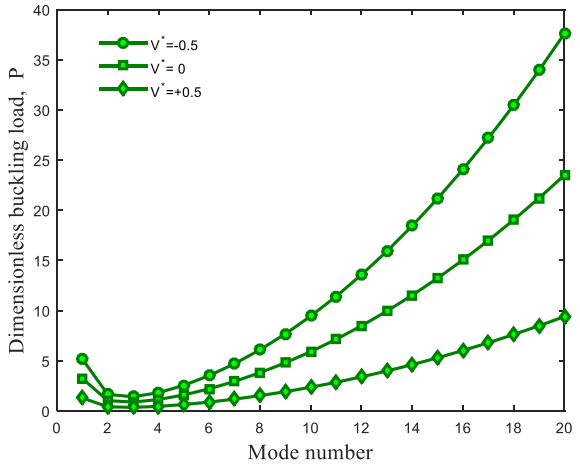

Fig. 4 External electric voltage effects on the dimensionless buckling load versus mode number

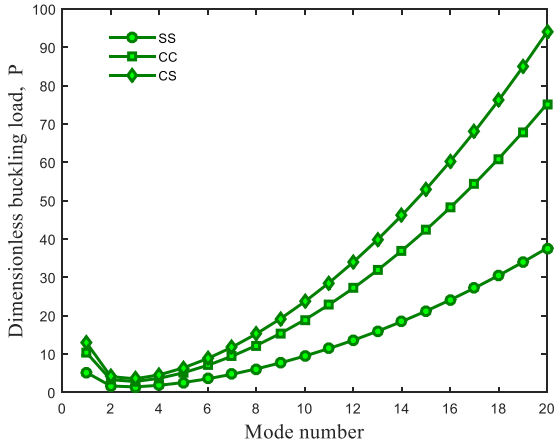

Fig. 6 Boundary condition effects on the dimensionless buckling load versus mode number

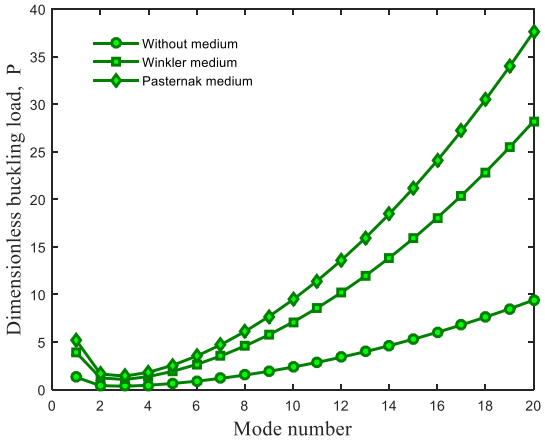

Fig. 5 Foundation effects on the dimensionless buckling load versus mode number

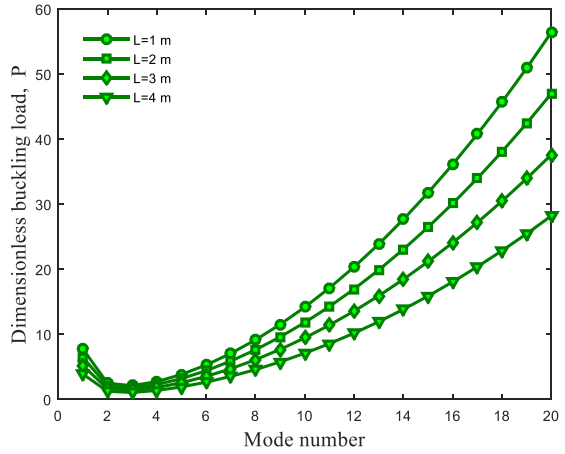

Fig. 7 The beam length effects on the dimensionless buckling load versus external electric voltage

Fig. 4 shows the dimensionless external applied voltage ($V^{*}=V_0/(h\sqrt{C_{11}/\in_{11}})$) effects on the dimensionless buckling load of beams versus the number of longitudinal mode. As can be seen, an applied negative external voltage causes to compressive force and increasing the buckling load of the system. This phenomenon is converse for positive external voltage. However, it can be concluded that applying external voltage is an effective controlling parameter for buckling behavior of smart beam.

Fig. 5 demonstrates the foundation effect on the dimensionless buckling load based on the number of longitudinal mode. Three types of foundation are considered namely as without foundation, modeling foundation with vertical springs (Winkler) and modeling foundation with vertical springs and shear layer (Pasternak). It can be seen that the buckling load of the beam is increased with considering foundation. In addition, the buckling load of the beam with Pasternak foundation is more than buckling of the beam with Winkler one. The reason for this is that in the model of Pasternak in addition to the flexibility factor, the effect of shear force is also considered.

Fig. 6 illustrates the effect of boundary conditions on the buckling load against the number of longitudinal mode. It can be found that the boundary conditions have a significant effect on the system buckling. In the beam with the clamped boundary conditions at both ends, buckling load is maximum with respect to other cases. The reason is that the CC boundary condition yields to maximum stiffness in structure with respect to other cases. In addition, the buckling load of beam with fixed-simple boundary condition is higher than Simple-Simple one.

Fig. 7 presents the dimensionless buckling load of structure versus mode number for different beam length. It is found that with enhancing the length of beam, the buckling load is decreased due to reduction in the stiffness

of structure.

5. Conclusions

In this study, buckling of embedded smart beams subjected to electric field was studied. The foundation was simulated by vertical springs and shear constants. The structure was modeled by SSDT mathematically. Using the strain-displacement equations, energy method and Hamilton's principal, the coupled governing equations was derived. Finally, using DQM, the buckling load of the structure was calculated and the effects of various parameters such as beam thickness and length, external voltage and the foundation were investigated on the buckling behavior of structure. Results indicate that the critical buckling load occurs in approximately third longitudinal mode. With increasing the beam thickness, the buckling load was increased. In general, existence of foundation increases the buckling load of structure. In addition, the boundary conditions have a significant effect on the beam buckling load. The results were validated with other published works.

“”

References

Alesadi, A., Galehdari, M. and Shojaee, S. (2017), “Free vibration and buckling analysis of cross-ply laminated composite plates using Carrera's unified formulation based on Isogeometric approach”, *Comput. Struct.*, **183**, 38-47, https://doi.org/10.1016/j.compstruc.2017.01.013.

Benahmed, A., Fahsi, B., Benzair, A., Zidour, M., Bourada, F. and Tounsi, A. (2019), “Critical buckling of functionally graded nanoscale beam with porosities using nonlocal higher-order shear deformation”, *Struct. Eng. Mech.*, **69**(4), 457-466, https://doi.org/10.12989/sem.2019.69.4.457.

Bilouei, B.S., Kolahchi, R. and Bidgoli, M.R. (2018), “Buckling of beams retrofitted with Nano-Fiber Reinforced Polymer (NFRP)”, *Comput.*, **18**(6), 1053-106, https://doi.org/10.12989/cac.2016.18.6.1053.

Eltaher, M.A. and Mohamed, S.A. (2020), “Buckling and stability analysis of sandwich beams subjected to varying axial loads”, *Steel Compos. Struct.,* **34**(2), 241-260. DOI: https://doi.org/10.12989/scs.2020.34.2.241.

Khelifa, Z., Hadji, L., Hassaine Daouadji, T. and Bourada, M., (2018), “Buckling response with stretching effect of carbon nanotube-reinforced composite beams resting on elastic foundation”, *Struct. Eng. Mech*., **67**(2), 125-130, https://doi.org/10.12989/sem.2018.67.2.125.

Kolahchi, R., Bidgoli, M.R., Beygipoor, G. and Fakhar, M.H. (2015), Free vibration and buckling analysis of cross-ply laminated composite plates using Carrera's unified formulation based on Isogeometric approach” *J. Mech. Sci. Technol.*, **29**, 3669-3677, https://doi.org/10.1007/s12206-015-0811-9.

Kolahchi, R., Hosseini, H. and Esmailpour, M. (2016a), “Differential cubature and quadrature-Bolotin methods for dynamic stability of embedded piezoelectric nanoplates based on visco-nonlocal-piezoelasticity theories”, *Compos. Struct.*, **157**, 174-186, https://doi.org/10.1016/j.compstruct.2016.08.032.

Kolahchi, R., Safari, M. and Esmailpour, M. (2016b), “Dynamic stability analysis of temperature-dependent functionally graded CNT-reinforced visco-plates resting on orthotropic elastomeric medium”, *Compos. Struct.*, **150**, 255-265, https://doi.org/10.1016/j.compstruct.2016.05.023.

Mehri, M., Asadi, H. and Wang, Q. (2016), “Buckling and vibration analysis of a pressurized CNT reinforced functionally graded truncated conical shell under an axial compression using HDQ method”, *Comput. Meth. Appl. Mech. Eng.*, **303**, 75-100, https://doi.org/10.1016/j.cma.2016.01.017.

Mosharrafian, F. and Kolahchi, R. (2016), “Nanotechnology, smartness and orthotropic nonhomogeneous elastic medium effects on buckling of piezoelectric pipes”, *Struct. Eng. Mech.,* **58**(5), 931-947, https://doi.org/10.12989/sem.2016.58.5.931.

Motezaker, M. and Eyvazian, A. (2020), “Post-buckling analysis of Mindlin Cut out-plate reinforced by FG-CNTs”, *Steel Compos. Struct.,* **34**(2), 289-297, https://doi.org/10.12989/scs.2020.34.2.289.

Motezaker, M. and Eyvazian, A. (2020), “Buckling load optimization of beam reinforced by nanoparticles”, *Struct. Eng. Mech.,* **73**(5), 481-486, https://doi.org/10.12989/sem.2020.73.5.481.

Mun, S. and Cho, YH. (2012), “Modified harmony search optimization for constrained design problems”, *Exp. Syst. Appl*., **39**, 419-423, https://doi.org/10.1016/j.eswa.2011.07.031.

Nejati, M., Eslampanah, A. and Najafizadeh, M. (2016), “Buckling and vibration analysis of functionally graded carbon nanotube-reinforced beam under axial load”, *Int. J. Appl. Mech.*, **8**, 1650008, 10.1142/S1758825116500083.

Thai, HT., and Vo, T.P. (2012), “A nonlocal sinusoidal shear deformation beam theory with application to bending, buckling, and vibration of nanobeams”, *Int. J. Eng. Sci.*, **54**, 58-66, https://doi.org/10.1016/j.ijengsci.2012.01.009.

Vodenitcharova, T. and Zhang, L. (2006), “Bending and local buckling of a nanocomposite beam reinforced by a single-walled carbon nanotube”, *Int. J. Solids Struct.*, **43**, 3006-3024, https://doi.org/10.1016/j.ijsolstr.2005.05.014.

Yang, J., Wu, H. and Kitipornchai, S. (2017), “Buckling and postbuckling of functionally graded multilayer graphene platelet-reinforced composite beams”, *Compos. Struct.*, **161**, 111-118. https://doi.org/10.1016/j.compstruct.2016.11.048.

Yas, M. and Samadi, N. (2012), “Free vibrations and buckling analysis of carbon nanotube-reinforced composite Timoshenko beams on elastic foundation”, *Int. J. Press. Vess. Pip.*, **98**, 119-128. https://doi.org/10.1016/j.ijpvp.2012.07.012.

Zamanian, M., Kolahchi, R., and Bidgoli, M.R., (2017), “Agglomeration effects on the buckling behaviour of embedded beams reinforced with SiO2 nano-particles”, *Wind. Struct.,* **24**(1), 43-57. https://doi.org/10.12989/was.2017.24.1.043.

CC